

Selective Etch for Micromachining Process in Manufacturing Hybrid Microdevices Composed of Ni-Mn-Ga and Silicon Layers

Hao Hu^{1,a*} Kari Ullakko^{1,b}

Lappeenranta-Lahti University of Technology, Finland

^ahuha0002@e.ntu.edu.sg, ^bkari.ullakko@lut.fi

Keywords: Microelectromechanical systems (MEMS), Ni-Mn-Ga, hybrid device, actuator, sensor, ferromagnetic shape memory, MSM, twinning.

Abstract. The goal of this study is to make selective etch possible for the next generation of MEMS (microelectromechanical systems) devices that are composed Ni-Mn-Ga and silicon layers. Due to the large magnetic-field-induced strains of Ni-Mn-Ga, sensing and actuating components can be fabricated in the Ni-Mn-Ga layers. Other functional components can be manufactured in the silicon layer. Single crystalline Ni-Mn-Ga alloys that are grown by using the Bridgman vertical growth technique have so far obtained the largest magnetic field-induced strain (MFIS), a magnetic shape memory (MSM) effect. Similar to silicon wafers, Ni-Mn-Ga wafers are also sliced from crystal-oriented single crystalline ingots. To fabricate hybrid MEMS devices such as micromanipulators and robots, lab-on-chip containing micropump manifolds and valves, or vibration energy harvesters, the fabrication processes used for MEMS devices will be also used to fabricate components in the Ni-Mn-Ga layer of the hybrid MEMS devices. One of the most important processes for MEMS fabrication is the structuring of materials by chemical etching. The main goal of this study is to obtain evidence that the etchant etches silicon but not Ni-Mn-Ga and to identify an etchant that etches Ni-Mn-Ga but not silicon. The present paper reports on a novel experiment in dissolving Ni-Mn-Ga alloys. An etchant composition of 69% HNO₃, 98% H₂SO₄, and CuSO₄•5H₂O is proposed for dissolving Ni-Mn-Ga alloys and the variation in the dissolution rate by adjusting the concentrations of HNO₃ and ultrapure water (UPW) is demonstrated. This etchant was demonstrated to etch Ni-Mn-Ga but not silicon. The HF+HNO₃ acidic solution commonly used for etching silicon does not dissolve Ni-Mn-Ga alloys.

Introduction

In recent years, nickel-manganese-gallium (Ni-Mn-Ga) based magnetic shape memory (MSM) alloys have attracted the attention of the industry due to their very high magnetic-field-induced strain (MFIS). The induced strain can be recovered by reorienting external magnetic field applied or by mechanical loading [1 – 3]. Unlike thermal shape memory effect, this MSM effect occurs within the martensitic phase, the key to which is the magnetic anisotropy of MSM alloys with tetragonal crystal structures [4 – 6]. Regions in the crystals with two different orientations of the short crystallographic c axis that are also along the natural direction of magnetization are called twin boundaries (TBs), illustrated as Fig. 1. During the magnetic-field-induced straining, the TBs move through the crystal until only one variant exists in the material. For the MSM effect to occur, low twinning stress and high energy magnetic anisotropy are required [5]. TB movement is inhibited significantly by the grain boundaries in polycrystalline materials; thus, researchers have also applied annealing for grain growth [6 - 8], compression [3, 9], and matching the grain and sample size [10] to enable high MFIS in polycrystalline Ni-Mn-Ga. Recently, MSM materials have been developed in the forms of single crystals, polycrystals, and nanowires [11 - 14] by using Bridgman vertical growth, additive manufacturing [15, 16], and electrodeposition. Increasingly more applications in robotics, biomedical, and optics use the Ni-Mn-Ga based MSM alloys such as fast actuators [17, 18], micropumps [19], and vibration energy harvesters [20].

Despite of the various developments of Ni-Mn-Ga based MSM alloys aiming at a large MSM effect, single crystalline Ni-Mn-Ga grown by using Bridgman vertical growth still prevails as the most

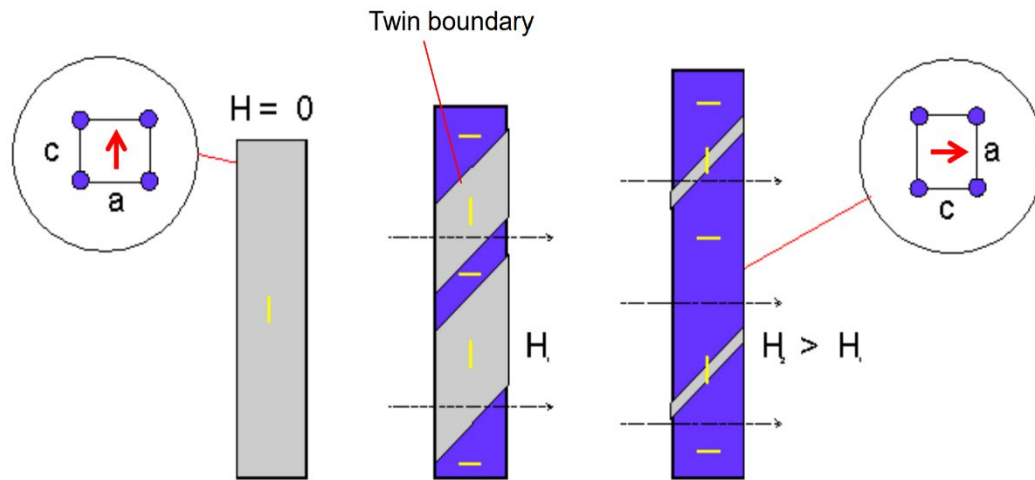


Fig. 1: The MSM phenomenon demonstrated in Ni-Mn-Ga. Twin boundary: there are regions in the crystals with two different orientations of the short crystallographic c axis, which is also along the natural direction of magnetization. (Modified from Publication [1])

effective technology in terms of the effect of MSM and the potential of mass production. In the semiconductor industry, microelectromechanical systems (MEMS) process technology [21 - 24] is applied to the manufacturing of micro- and nanostructured electronic devices, high-precision components, and micro biosensors. This technology allows for the manufacturing of micro-sized devices and high-precision components with better electrical performance, improved thermal management, and reliable functionality at lower cost and smaller package size. In the past two decades, researchers have worked intensively to advance the MSM materials and their performance. Applying the well-known fabrication processes used in the semiconductor industry, such as selective etching, ion implantation, polishing, and lithography, may offer new methods of MSM fabrication. The proposed process flow of MSM wafer fabrication is illustrated as Fig. 2. Meanwhile, microprocessing of MSM alloys enhance further the working frequency owing to its little hysteresis and high reversibility [26]. The goal is to develop MSM hybrid microdevices that are composed of a Ni-Mn-Ga material layer and a Si layer. These layers are structured using etching and lithographic methods to manufacture actuating, sensing, and functional components in the device. Components fabricated in the Ni-Mn-Ga layers can be as the active regions of actuators, sensors, pumps, valves or grippers [25, 27]. Thus it is essential to make selective etch for micromachining process in manufacturing hybrid microdevices composed of both Ni-Mn-Ga and silicon layers. The primary task of this paper is to find such a chemical etchant that dissolves Ni-Mn-Ga but not Si, and to identify a chemical etchant ($\text{HF}+\text{HNO}_3$) that selectively etches Si but does not dissolve Ni-Mn-Ga. With these motivations in mind, the investigations reported in the present paper aim to achieve the following tasks:

1. To confirm by the experiment that the etchant, an $\text{HF}+\text{HNO}_3$ acid solution, often used as the chemical solution (selective etch) for silicon, does not dissolve the Ni-Mn-Ga single-crystal sample investigated.
2. An etchant dissolving the Ni-Mn-Ga sample will be identified, and to confirm by the experiment that the etchant for Ni-Mn-Ga dissolution does not dissolve silicon (dissolution rate $< 10 \text{ mg/min}$).
3. The chemical reaction of Ni-Mn-Ga sample with the different compositions of the etchant consisting of H_2SO_4 , HNO_3 and CuSO_4 will be elucidated.
4. The optimized composition of the etchant for dissolving the Ni-Mn-Ga sample will be identified.

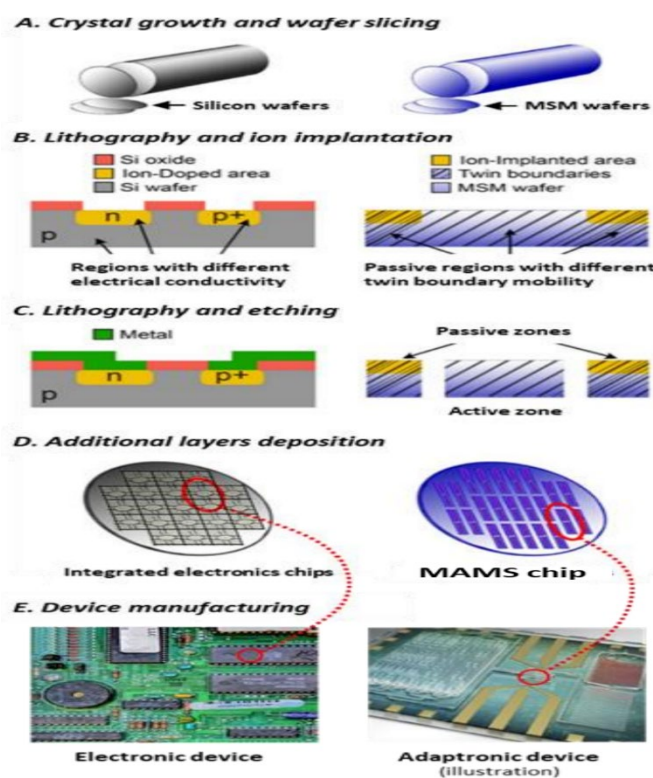


Fig. 2: Proposed MSM device fabrication process that similar to integrated circuit fabrication on silicon wafers

Experimental Details

A single crystalline Ni-Mn-Ga alloy rod with a diameter of 10 mm and a length of 50 mm was cut into slices with a weight in the range from 0.5 g to 2 g. The slices were added to chemical solutions with different compositions or varied concentrations of the etchant (69% HNO_3 , 98% H_2SO_4 , and $\text{CuSO}_4 \cdot 5\text{H}_2\text{O}$) at room temperature.

The dissolution rate was calculated according to the weight of the sample versus the time of complete dissolution. The sample and experimental parameters are summarized in Tables 1 and 2. To accomplish the abovementioned goals, four experiments were performed as follows:

A. Etching of Si and Ni-Mn-Ga samples with $\text{HF} + \text{HNO}_3$ acid solution

In Experiment 1, a small piece of the Si Boron-doped p-type (100) sample, with the resistivity of 18–25 $\Omega \cdot \text{cm}$, a weight of 1.39 grams and a Ni-Mn-Ga sample with a weight of 1.56 grams was used. An etchant formed by combining 50% HF (10 ml) and 55% HNO_3 (10 ml) supplied by Tama Chemicals was used. The Si and Ni-Mn-Ga samples were cleaned by rinsing in ultrapure water (UPW) before etching. UPW had metal traces lower than 1 ng/L inspected routinely on an ICP-MS7500 (Agilent).

B. Etching Si and Ni-Mn-Ga samples with an aqueous solution of HNO_3 , H_2SO_4 , and $\text{CuSO}_4 \cdot 5\text{H}_2\text{O}$ In Experiment 2, an etchant containing nitric acid (HNO_3), sulfuric acid (H_2SO_4), and copper (II) sulfate pentahydrate ($\text{CuSO}_4 \cdot 5\text{H}_2\text{O}$) was tested for dissolving Ni-Mn-Ga alloys. An aqueous solution containing 69% HNO_3 (25 ml), 98% H_2SO_4 (3.5 ml), and $\text{CuSO}_4 \cdot 5\text{H}_2\text{O}$ (7.5 g) was used and illustrated as Composition B in Table 1 and Fig. 3. The chemicals used were supplied by Sigma-Aldrich. A Si sample weighing 1.44 g and a Ni-Mn-Ga sample weighing 1.66 g were used in this experiment.

C. Rate of Ni-Mn-Ga dissolution with etchants of different compositions.

To develop actuating or sensing components in the Ni-Mn-Ga layer of the hybrid device, the rate of the Ni-Mn-Ga alloy etching must be controlled. Such control may be achieved by changing the ratio of the chemicals in the etchant. Experiment 3 aimed to demonstrate the reactions of the Ni-Mn-Ga sample with different etchants, illustrated as Composition A, B, C and D in Fig. 3. Four compositions were tested at room temperature (23 °C).

D. Fine tuning of the rate of dissolution of Ni-Mn-Ga alloy.

In this experiment, the amount of H_2SO_4 and $\text{CuSO}_4 \cdot 5\text{H}_2\text{O}$ was held constant, whilst the amounts of HNO_3 and UPW in the etchant were systematically varied in four steps, referred to as Tests 1 to 4 in Table 2.

Table 1: Experimental details and parameters of composition of etchant (A-E) Experiment

Experiment	Weight of Ni-Mn-Ga	Dissolution rate of Ni-Mn-Ga	Composition of Etchant
1	1.56 g	6 mg/min	E
2	1.66 g	121 mg/min	B
3	0.58 g	127 mg/min	A
	1.65 g	121 mg/min	B
	0.95 g	174 mg/min	C
	0.62 g	6 mg/min	D

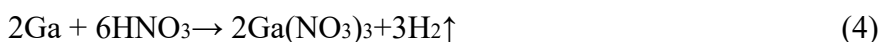
Results and Discussion

In Experiment 1, Si reacted to the chemical solution of HNO_3 and HF, as shown in Eq 1.

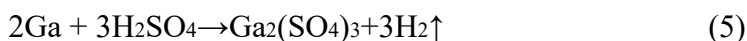


Illustrated as Composition E in Table 1, with a combination of 50% HF (10 ml) and 55% HNO_3 (10 ml), the rate of dissolution of the Si sample was found to be 120 mg/min, whereas that of the Ni-Mn-Ga sample was less than 6 mg/min, illustrated as Experiment 1 in Table 1. It concluded that the Ni-Mn-Ga sample did not react effectively with this etchant and remained unetched in the Si etching process commonly used in semiconductor fabrication [27 - 29]. The result of Experiment 2 confirmed that the solution made from 69% HNO_3 , 98% H_2SO_4 , and $\text{CuSO}_4 \cdot 5\text{H}_2\text{O}$ dissolved Ni-Mn-Ga but did not etch Si. No obvious reaction with Si was observed during the test. However, this etchant effectively dissolved the Ni-Mn-Ga sample with a rate of 121 mg/min. The following chemical reactions were observed:

Nitric acid (HNO_3) reacted with nickel, manganese, and gallium to form nickel (II) nitrate, manganese (II) nitrate, and gallium (III) nitrate, respectively, and also to generate hydrogen gas. The reactions are shown as Eq. 2 - 4.



Sulfur acid and sulfur-containing species are the good stabilizing agents in this application. During the experiments, the color of the solution changed due to the reaction of Ni (green) and of manganese (yellow) with the sulfuric acid. Gallium is often used as a semiconductor material and is soluble in most of acids and bases. Gallium sulfate, nickel sulfate, and manganese sulfate were formed as shown in Eq. 5 - 7.



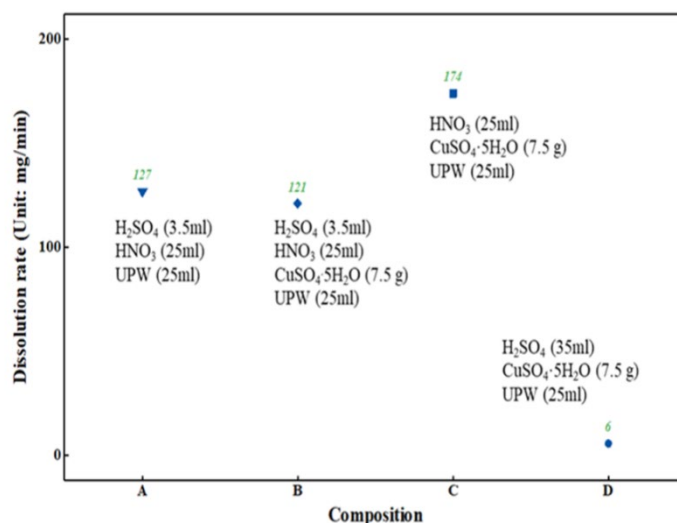
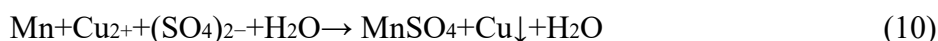


Fig. 3: Dissolution rate of Ni-Mn-Ga denoted by the green numbers, mg/min based on the chemical composition of the etchant



Copper (II) sulfate pentahydrate ($\text{CuSO}_4 \cdot 5\text{H}_2\text{O}$), a bright blue crystalline solid, is a hydrate and a metal sulfate that contains copper (II) sulfate. It acts as the stabilizing agent in the reaction with Cu particles, catalyzing the reaction. It also helps to tune the dissolution rate. The detailed reactions are shown in Eq. 8 - 10.



In Experiment 3, using Composition D, the Ni-Mn-Ga sample was not dissolved effectively, as the dissolution rate was less than 10 mg/min. The dissolution rate ranged from 121 mg/min to 174 mg/min when Compositions A, B, and C were used, as illustrated in Fig. 3.

Selecting Composition B as the etchant for Ni-Mn-Ga dissolution, Experiment 4 was conducted to fine tune the composition of the etchant by varying the relative concentrations of the involved chemicals. Four tests, denoted as Tests 1, 2, 3 and 4, were performed on the Ni-Mn-Ga sample. The details of these tests and the results are shown in Table 2 and Fig. 4.

Table 2: Rate of dissolution of the Ni-Mn-Ga sample with different ratios of chemicals in the etchant. Chemical composition B : 69% HNO₃, 98% H₂SO₄, CuSO₄·5H₂O and UPW

	Test 1	Test 2	Test 3	Test
4 98% H ₂ SO ₄	3.5 ml	3.5 ml	3.5 ml	3.5
ml 69% HNO ₃	25 ml	30 ml	25 ml	30
ml CuSO ₄ ·5H ₂ O	7.5 g	7.5 g	7.5 g	7.5
g UPW	25 ml	25 ml	50 ml	50
ml Dissolution rate (mg/min)	122	145	87	102

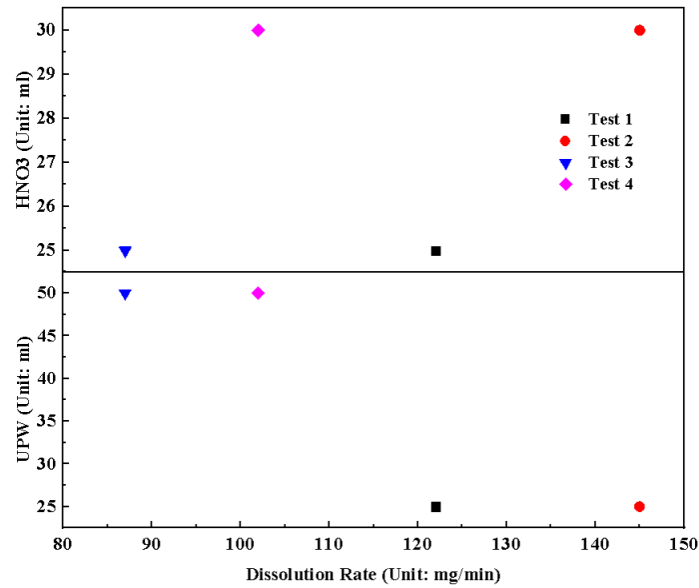


Fig. 4: Change in the dissolution rate of Ni-Mn-Ga with the adjustment of HNO₃ and UPW. The amount of HNO₃ was increased from 25 ml (Tests 1 and 3) to 30 ml (Tests 3 and 4); the amount of UPW was doubled from 25 ml (Tests 1 and 2) to 50 ml (Tests 3 and 4).

Composition B resulted in a similar dissolution rate of the Ni-Mn-Ga sample, shown as Test 1 in Table 2, that of the Si sample in Experiment 1 (120 mg/min) with a combination of 50% HF (10 ml) and 55% HNO₃ (10 ml). In Test 2, the amount of nitric acid (69% HNO₃) was increased in volume by 20%. As a result of this modification, the dissolution rate increased to 145 mg/min from 122 mg/min. In Tests 3 and 4, the UPW volume was doubled with respect to the volume used in Tests 1 and 2. When the etchant was diluted, the dissolution rate was reduced to 87 mg/min (Test 3) from 122 mg/min (Test 1), and from 145 mg/min (Test 2) to 102 mg/min (Test 4). Therefore, the rate of dissolution of the Ni-Mn-Ga sample in the etchant (69% HNO₃, 98% H₂SO₄, and CuSO₄•5H₂O) can be adjusted by modifying the concentrations of the nitric acid or the amount of added UPW. Applying the technology of the semiconductor MEMS micromachining process gives huge flexibility of making complex smart devices that composited of Ni-Mn-Ga alloy as the sensing or actuating components, the active region, thus the inactive regions such as housing, mechanical support, and structures can be fabricated using the standard MEMS micromachining process. Ullakko[30] proposed the approach to develop the MSM devices that consist of the regions of active and inactive, illustrated as in Fig. 5. In the approach, the

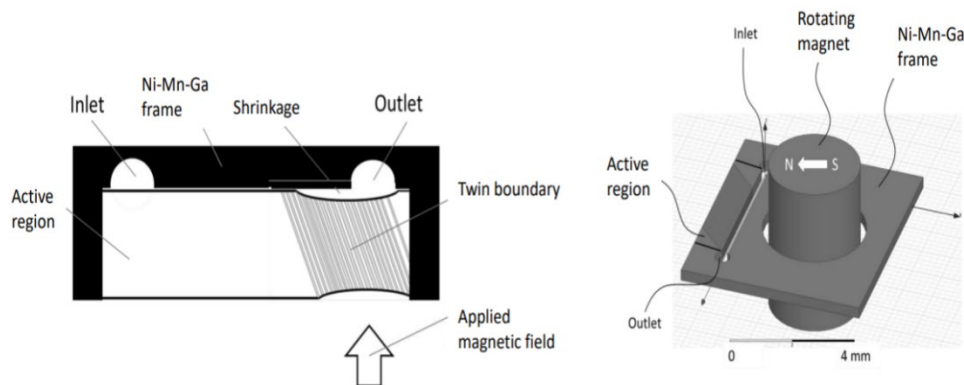


Fig. 5: An example of MSM parts made inclusive of active region (Ni-Mn-Ga) and inactive region. (Source from Publication [30])

sensing or actuating part is developed by using Ni-Mn-Ga alloy, and the housing or other functioning part is made from other materials such as Si substrate. The Ni-Mn-Ga region will be driven by the external magnetic fields.

Conclusions

It was demonstrated that an etchant formed from 69% nitric acid, 98% sulfuric acid, and copper (II) sulfate pentahydrate effectively dissolved the Ni-Mn-Ga alloy sample, but it did not dissolve the Si sample. In contrast, the HF/HNO₃ acid solution commonly used for etching Si did not substantially dissolve the Ni-Mn-Ga alloy sample. The results of the experiments presented in this report also illustrated the variations in the rate of Ni-Mn-Ga dissolution with the adjustment of the concentration of nitric acid and amount of added ultrapure water. This result suggests that selective etching, a technology that is also used in semiconductor fabrication, may be possible for Ni-Mn-Ga alloys. These results on selectively etching Si and Ni-Mn-Ga form the basis for developing MSM hybrid microdevices composed of a Ni-Mn-Ga material layer and Si layer, meanwhile, trigger the demand for developing further the micromachining processes for fabricating Ni-Mn-Ga layer such as cleaning, annealing, lithography and bonding.

CRedit authorship contribution statement

Hao Hu: Investigation, Writing, Project administration. Kari Ullakko: Writing-Review, Supervision.

Acknowledgements

The authors thank Analytical Test Centre of Chongqing Institute of Green and Intelligent Technology, Chinese Academy of Sciences for providing the laboratory facility.

References

- [1] K. Ullakko, J. Huang, C. Kantner, R. Handley, V. Kokorin, Large magnetic-field induced strain in Ni₂MnGa single crystals, *Applied Physics Letters*, (1996), 69, 1966-1968.
- [2] P. Zheng, P. Lindquist, B. Yuan, P. Müllner, D. Dunand, Fabricating Ni-Mn-Ga microtubes by diffusion of Mn and Ga into Ni tubes, *Intermetallics*, (2014), 49, 70-80.
- [3] R. Chulist, E. Pagounis, P. Czaja, N. Schell, H. Brokmeier, New Insights into the intermartensitic transformation and over 11 % magnetic-field-induced strain in 14 m Ni-Mn-Ga martensite, *Advanced Engineering Materials*, (2021), 23, 2100131(1-6).
- [4] J. Pons, V. Chernenko, R. Santamarta, E. Cesari, Crystal structure of martensitic phases in Ni-Mn-Ga shape memory alloys, *Acta Materialia*, (2000), 48, 3027-3038.
- [5] A. Likhachev, K. Ullakko, Magnetic-field-controlled twin boundaries motion and giant magneto-mechanical effects in Ni-Mn-Ga shape memory alloy, *Physics Letters A*, (2000), 275, 142-151.
- [6] I., Kulagin, M. Li, L. Ville, H. Heikki, Review of MSM actuators: applications, challenges, and potential, *IEEE Access*, (2022), 10, 83841-83850.
- [7] U. Gaitzsch, J. Drache, K. McDonald, P. Müllner, P. Lindquist, Obtaining of Ni-Mn-Ga magnetic shape memory alloy by annealing electrochemically deposited Ga / Mn / Ni layers, *Thin Solid Films*, (2012), 522, 171-174.
- [8] H. Lei, L. Tong, Z. Wang, Effect of temperature on magnetic field – induced response of Ni-Mn-Ga single crystals, *Journal of Intelligent Material Systems and Structures*, (2015), 26, 2395-2410.
- [9] P. Polyakov, V. Slyusarev, V. Kokorin, S. Konoplyuk, Y. Semenova, V. Khovaylo, Volume change during intermartensitic transformations in Ni-Mn-Ga alloy, *Journal of Materials Engineering and Performance*, (2014), 23, 3180-3183.
- [10] D. Dunand, P. Müllner, Size effects on magnetic actuation in Ni-Mn-Ga shape memory alloys, *Advanced Materials*, (2011), 23, 216-232.

-
- [11] B. Özkale, F. Mushtaq, J. Fornell, G. Chatzipirpiridis, L. Martin, J. Sort, C. Müller, E. Pellicer, B. Nelson, S. Pané, Single step electrosynthesis of NiMnGa alloys, *Electrochimica Acta*, (2016), 204, 199-205.
 - [12] K. Javed, X. Zhang, S. Parajuli, S. Ali, N. Ahmad, S. Shah, M. Irfan, J. Feng, Magnetization behavior of NiMnGa alloy nanowires prepared by DC electrodeposition, *Journal of Magnetism and Magnetic Materials*, (2020), 498, 166232.
 - [13] Y. Zhang, F. Qin, D. Estevez, V. Franco, H. Peng, Structure, magnetic and magnetocaloric properties of Ni₂MnGa Heusler alloy nanowires, *Journal of Magnetism and Magnetic Materials*, (2020), 513, 167100.
 - [14] S. Hutagalung, M. Fadhal, R. Areshi, F. Tan, Optical and electrical characteristics of silicon nanowires prepared by electroless etching, *Nanoscale Research Letters*, (2017), 12, 425-436.
 - [15] V. Laitinen, A. Saren, A. Sozinov, K. Ullakko, Giant 5.8 % magnetic-field-induced strain in additive manufactured Ni-Mn- Ga magnetic shape memory alloy, *Scripta Materialia*, (2022), 208, 114324 (2022).
 - [16] A. Mostafaei, K. Kimes, E. Stevens, J. Toman, Y. Krimer, K. Ullakko, M. Chmiel, Microstructural evolution and magnetic properties of binder jet additive manufactured Ni-Mn-Ga magnetic shape memory alloy foam, *Acta Materialia*, (2017), 131, 482-490.
 - [17] A. Smith, J. Tellinen, K. Ullakko, Rapid actuation and response of Ni-Mn-Ga to magnetic-field-induced stress, *Acta Materialia*, (2014), 80, 373-379.
 - [18] K. Ullakko, Magnetically controlled shape memory alloys: a new class of actuator materials, *Journal of Materials Engineering and Performance*, (1996), 5, 405-409.
 - [19] K. Ullakko, L. Wendell, A. Smith, P. Müllner, G. Hampikian, A magnetic shape memory micropump: contact-free, and compatible with PCR and human DNA profiling, *Smart Materials and Structures*, (2012), 21, 115020 (1-10).
 - [20] A. Saren, D. Musienko, A. Smith, J. Tellinen, K. Ullakko, Modeling and design of a vibration energy harvester using the magnetic shape memory effect, *Smart Materials and Structures*, (2015), 24, 95002.
 - [21] V. Lindroos, M. Tili, A. Lehto, T. Motooka, Handbook of Silicon Based MEMS Materials and Technologies, William Andrew, (2010), 636 .
 - [22] H. Qu, CMOS MEMS fabrication technologies and devices, *Micromachines*, (2016), 7, 1-21.
 - [23] R.A. Moghadam, H. Saffari, J. Koohsorkhi, Ni-P electroless on nonconductive substrates as metal deposition process for MEMS fabrication, *Microsystem Technologies*, (2021), 27, 79-86.
 - [24] R. Anthony, N. Wang, D. Casey, C. Mathúna, J. Rohan, MEMS based fabrication of high-frequency integrated inductors on Ni-Cu-Zn ferrite substrates, *Journal of Magnetism and Magnetic Materials*, (2016), 406, 89-94.
 - [25] A. Algamili, M. Khir, J. Dennis, A. Ahmed, S. Alabsi, S.B. Hashwan, M. Junaid, A review of actuation and sensing mechanisms in MEMS-based sensor devices, *Nanoscale Research Letters*, (2021), 16, 1-21.
 - [26] X. Zhang, M. Qian, Magnetic shape memory alloys - preparation, martensitic transformation and properties, Harbin Institute of Technology Press, (2022), 1200.
 - [27] K. Williams, R. Muller, Etch rates for micromachining processing, *Journal of Microelectromechanical Systems*, (1996), 5, 256-269.
 - [28] K. Williams, K. Gupta, M. Wasilik, Etch rates for micromachining processing - Part II, *Journal of Microelectromechanical Systems*, (2003), 12, 761-778.
 - [29] B. Wu, A. Kumar, S. Pamarthy, High aspect ratio silicon etch: a review. *Journal of Applied Physics*, (2010), 108, 051101.
 - [30] K. Ullakko, Operation element comprising magnetic shape memory alloy and a method for manufacture it. U.S. Patent PCT/FI2019/050613, PAT 1388 WO.